A Fiber Optic Sensor for Cracks in Concrete Structures

Christopher K.Y. Leung, K.T. Wan
Hong Kong University of Science and Technology, Hong Kong, China SAR

Y. Jiang
Beijing Institute of Technology, Beijing, China

ABSTRACT: The condition of a concrete structure can be effectively assessed through the monitoring of cracks. Large cracks may be warning signs of severe degradation, while small cracks with openings from 0.2 to 0.4 mm may lead to durability problems associated with the penetration of water and other chemicals. In this presentation, we will describe recent developments on a fiber optic crack sensor that allows the detection and monitoring of multiple cracks without requiring prior knowledge of crack locations. After a discussion of the sensing principle, a theoretical model for signal loss vs crack opening is derived to provide guidelines for sensor design. The fabrication of a sensor suitable for both external bonding and internal installation in a concrete structure will then be described. Representative experimental results will be shown and comparison with theoretical predictions is conducted. Based on the experimental and theoretical findings, the potential of the sensor for practical applications is demonstrated.

Keywords: cracks, fiber optic sensing, monitoring, non-destructive evaluation

1 INTRODUCTION

The degradation of concrete structures is a major infrastructure problem in many parts of the world. If deterioration can be detected at an early stage, timely maintenance can extend the lifetime of structures, and avoid severe degradation that may jeopardize public safety. Due to the low tensile strength of concrete, deterioration is always accompanied by the formation and propagation of cracks. The condition or "health" of a concrete structure is hence best assessed from its state of cracking. For example, if cracks in a concrete structure open by more than 0.2 to 0.4 mm under service loading, penetration of water and salt (from sea water) will accelerate the corrosion of steel. Once such cracks are detected, they should be sealed. Crack monitoring is also an effective means to assess structural condition after the occurrence of natural hazards. After a strong earthquake, if widely opened cracks (of several mm's) are detected at critical locations, the structure is likely to be severely damaged, and should be closed down for repair.

Due to material inhomogeneities, the exact locations of cracks in a concrete structure cannot be predicted. Conventional sensors are either point sensors (such as strain gauges and accelerometers) that only provide information at a single point of the structure, or integrated sensors (e.g, a LVDT with long gauge length) that measure displacement between two points separated by a relatively large distance. Since cracks in reinforced concrete structures have little effect on overall structural stiffness, the displacement, strain or acceleration at a particular sensing point is insensitive to cracking unless the point is very close to the damage location. If point sensors are employed, the required number of sensors to guarantee the detection of each potential crack will be excessively large for any monitoring scheme to be practical. On the other hand, if integrated sensors are used, it is not possible to distinguish between displacement due to creeping or cracking. Also, one cannot tell between the harmless condition of many fine cracks and the undesirable situation of one widely opened crack.

To overcome the limitations of conventional sensors, Leung et al. (2000, 2001) have developed a novel distributed crack sensor based on the optical fiber. Since the fiber can act as both the sensor and the communication link, it can theoretically detect any changes taking place along its length. If the optical fiber is coupled to a concrete structure in a proper way, any crack that forms along the fiber can be detected, and a single fiber is able to detect and monitor a number of cracks. In the following sections, the sensing principle is first explained. Then, recent theoretical and experimental investigations on this sensing concept will be described.

2 SENSING PRINCIPLE

The principle of the sensor is illustrated in Figure 1a, which shows a 'zig-zag' optical fiber coupled to the concrete member. The backscattered power is measured as a function of time with Optical Time Domain Reflectometry (OTDR). Before the formation of cracks, the backscattered signal vs. time follows a relatively smooth curve (the upper line in Figure 1b). The gradual loss in signal power with time is due to the increased distance traveled by the light signal. In the curved portion (where the fiber changes in direction), bending loss may occur depending on the radius of curvature. If the sensor geometry is designed to have a small curvature at the turning point, this loss will be negligible. When a crack opens in the structure, a fiber intersecting the crack at an angle other than 90° has to bend to stay continuous (see inset of Fig. 1a). The sudden bending of an optical fiber at the crack results in a sharp drop in the optical signal (lower line, Fig. 1b). From the times corresponding to the sharp signal drops in the OTDR record, the location of each crack in the structure can be easily calculated as the light velocity in the optical fiber is known. From the magnitude of each drop, the crack opening can be determined.

The proposed technique does not require prior knowledge of the crack locations. However, crack directions need to be known. This is usually not a problem because cracks normally run perpendicularly to the principal tensile direction, which can be obtained from structural analysis.

To sense cracks effectively, several sensors should be employed. With a single fiber, if a crack intersects the 'zig-zag' fiber at a location where the fiber direction is changing, results will be difficult to interpret. The crack therefore needs to be picked up by another fiber with its turning point at other sections. Depending on the application, the sensor can either be cast inside the concrete, or bonded to the surface of the concrete member.

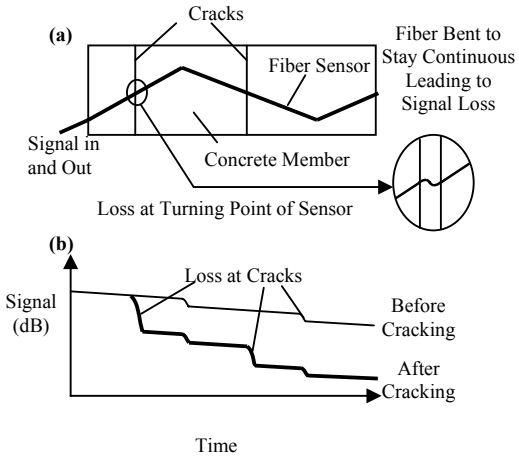

Figure 1. Concept of Distributed Sensing with the Novel Sensor

In designing the sensor, the signal loss vs. crack opening relation needs to be optimised. High loss at small crack openings would increase the sensitivity of crack detection. However, since the dynamic range of OTDR measurement is limited, high loss at each crack will limit the total number of cracks that can be detected and monitored with a single fiber. For a given crack opening, the signal loss depends on many parameters including (i) the optical properties of the fiber, (ii) the fiber inclination angle to the crack, and (iii) the elastic properties of the fiber, the surrounding matrix and the protective polymeric coating on the fiber. In the following section, a model for signal loss vs. crack opening is developed to provide guidelines for sensor design.

3 DERIVATION OF A THEORETICAL MODEL FOR POWER LOSS

The analysis of the optical power loss in the crack sensor involves two major steps. As the crack opens, the induced curvature along the fiber is first obtained through a mechanical analysis. An optical analysis is then performed to compute the power loss along the curved waveguide.

A model for the mechanical analysis is shown schematically in Figure 2. It is assumed that the

influence of the matrix surrounding the optical fiber occurs within five fiber diameters from the fiber center. From preliminary analysis, this is found to be sufficient to simulate a matrix of infinite extent. The fiber length on each side of the crack was taken to be about 36 times the fiber diameter, which is adequate for the fiber to return to an essentially straight configuration. The dotted lines in Figure 2a show the part of the matrix that will be included in a three-dimensional finite element analysis. Figure 2b and 2c illustrate the loading and boundary conditions of the analysis. The crack opening is assumed to be made up of two parts, a displacement component u_1 parallel to the fiber as in Figure 2b, and a perpendicular component u_2 that would bend the fiber into a curved configuration. The magnitude of the two components can be easily calculated from the actual opening of the crack (δ) and the angle between fiber and crack opening direction (θ) as:

$$u_1 = \delta \cos\theta \quad (1)$$

$$u_2 = \delta \sin\theta \quad (2)$$

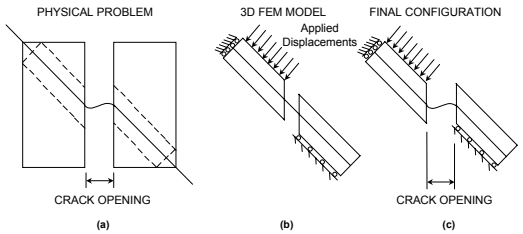

Figure 2. Schematic Illustration of the Mechanical Analysis

As can be observed in Figure 2c, when the fiber inclination is high, the part of fiber between the crack faces may rotate significantly from its original orientation. A large displacement analysis should therefore be performed. Initial work with large displacement analysis of the problem reveals that the computation time is very long, and convergence is not achievable in many cases. In view of the fact that the purpose of the modeling work is to provide approximate results to guide the design of sensors, we revert to small displacement finite element stress analysis. However, the effect of large displacement is not completely neglected. After obtaining the displacements from the analysis (which assume small displacement in the stiffness matrix formulation), the fiber curvature is calculated from $d\theta/ds$ rather than $d\theta/dx$, where $d\theta$ is the change of rotation between two points, dx is the distance between the two points in the un-deformed configuration, and ds is the distance in the deformed configuration. The validity of this approximate approach will be justified by comparison with experimental results in a later section.

To perform the finite element analysis, the ADINA program was employed. Twenty-node three-dimensional solid elements were used to model the fiber, the matrix as well as the polymeric coating around the fiber. The elastic properties of the fiber and matrix are well known, while that of the fiber coating was measured with the nano-indentation technique (Olson et al. 2002). In the analysis, 8,400 20-node solid elements were employed. Figure 3 shows the finite element mesh near the crack opening. Where there is tensile normal stress along the fiber coating/matrix interface, a thin layer of material with very low modulus value (several orders below that of polymer) is prescribed. This layer, marked as "Separation Zone" in Figure 3, allows for the separation of the fiber as it is bent away from the matrix. When the fiber is bent on the matrix, the deformed shape is like a damped sinusoidal curve, so the separation zone alternates from one side to the other side. The actual extent of each separation zone needs to be obtained from iteration. Since the extent of the separation zone is also a function of the crack opening. Therefore, for each crack opening and fiber inclination angle, a number of iterations are required to get the final result.

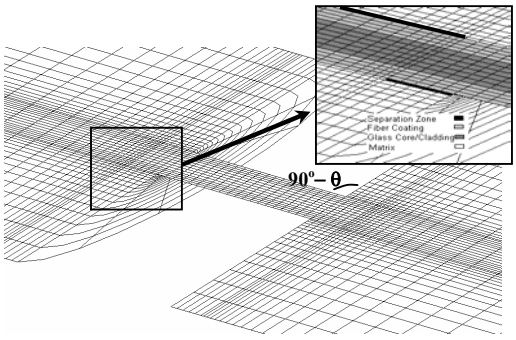

Figure 3. Typical Finite Element Mesh around the Crack

To improve the efficiency of the analysis, a simplification is made. Instead of having separation zones on both sides of the fiber, we put it on one side of the fiber only. Iteration on the separation zone size is then no longer necessary. Numerical

results from finite element analysis showed that the simplified approach produced results very close to that of the former approach, which requires iteration. With a single separation zone, the problem can be further simplified as in Figure 4a. The parts of fiber inside and outside the matrix are considered separately. As shown in Figure 4a, when a force (F) is applied to the end of a fiber coming out from the matrix, the total displacement (u) can be expressed as:

$$u = u_o + L\theta_o + \frac{FL^3}{3EI} \tag{3}$$

where u_o and θ_o are respectively the displacement and rotation at the center of the fiber section above the point of entry into the matrix (see Fig. 4b), and EI is the equivalent fiber stiffness (which includes the stiffness of both the glass fiber and the fiber coating). Also,

$$\begin{bmatrix} u_o \\ \theta_o \end{bmatrix} = \begin{bmatrix} u_F & u_M \\ \theta_F & \theta_M \end{bmatrix} \begin{bmatrix} F \\ FL \end{bmatrix} \tag{4}$$

with F and FL being the shear force and moment acting on the embedded part of the fiber respectively.

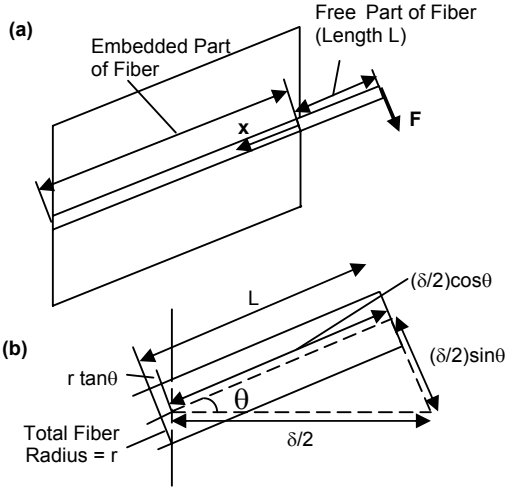

Figure 4. (a) Separating the Optical Fiber into Free Part and Embedded Part (b) Geometric Relation between Crack Opening and Free Fiber Length

More generally, we can define u(x) to be the transverse displacement along the embedded part of the fiber, as a function of distance (x) from the fiber entry point. Similarly, θ(x) can be defined as the fiber rotation which is a function of distance (x). Equation 4 can then be generalized into:

$$\begin{bmatrix} u(x) \\ \theta(x) \end{bmatrix} = \begin{bmatrix} u_F(x) & u_M(x) \\ \theta_F(x) & \theta_M(x) \end{bmatrix} \begin{bmatrix} F \\ FL \end{bmatrix} \tag{5}$$

with u(0) = u_o and θ(0) =θ_o. The functions $u_F(x)$, $u_M(x)$, $\theta_F(x)$ and $\theta_M(x)$ correspond to the effect of unit force or moment acting at the point where the fiber enter the matrix. To obtain these four functions in a numerical manner, analyses can be performed with two independent finite element analyses using two different values of fiber free length (L). For example, if analyses is performed with L = L_1 and L_2,

$$u(x)|_{L=L_1} = u_F(x)F + u_M(x)FL_1 \tag{6a}$$

$$u(x)|_{L=L_2} = u_F(x)F + u_M(x)FL_2 \tag{6b}$$

From Equations 6a and 6b, it is clear that $u_F(x)$ and $u_M(x)$ can be obtained once the displacement distributions u(x) from the two separate analyses are known. Similarly, from

$$\theta(x)|_{L=L_1} = \theta_F(x)F + \theta_M(x)FL_1 \tag{7a}$$

$$\theta(x)|_{L=L_2} = \theta_F(x)F + \theta_M(x)FL_2 \tag{7b}$$

$\theta_F(x)$ and $\theta_M(x)$ can be determined.

Knowing $u_F(x)$, $u_M(x)$, $\theta_F(x)$ and $\theta_M(x)$, the fiber curvature distribution for any crack opening can be easily obtained. Assume the fiber to be cut at a location half way between the two crack faces. When the crack opens, the middle of the fiber section at the cut end must deform to the same level as the fiber axis at the crack surface. Also, due to anti-symmetry, there is no moment but only transverse force acting on the cut end. To fit the two sides of the fiber back together, the transverse force must produce a displacement equal to (δ/2) sinθ, where δ/2 is half the total crack opening, and θ is the fiber inclination angle. Also, the free fiber length is given by:

$$L = (\delta/2)\cos\theta + r\tan\theta \tag{8}$$

In Equation 8, r is the total radius of the fiber (including the glass fiber as well as the protective coating as shown in Fig. 4b). Knowing the free fiber length (from Equation 8) and the required displacement to fit the two sides of the fiber together, the transverse force F can be calculated from Equation 3. Then, with F and FL, u(x) and θ(x) along the embedded part of the fiber can be obtained. It should be noted that the curvature

distribution along the curved part should be calculated from dθ/ds, where s the distance between adjacent points in the deformed configuration, rather than dθ/dx, because the displacement can be quite large in some cases. This approach is consistent with the derivation of curvature from the finite element results.

With the original finite element analysis, a full 3-D analysis has to be performed for each crack opening. With the semi-analytical approach described above, the finite element analysis only needs to be run twice for each crack opening to obtain the coefficients $u_F(x)$, $u_M(x)$, $\theta_F(x)$ and $\theta_M(x)$. The displacement and curvature distribution for any crack opening can then be obtained analytically.

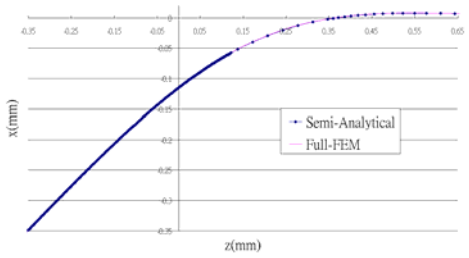

Figure 5. Displacement along a Fiber from the Full FEM Model and the Semi-Analytical Approach of 3M 45 at 2mm crack opening

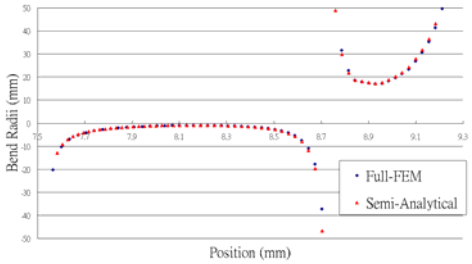

Figure 6. Raius of curvature along a Fiber from the Full FEM Model and the Semi-analytical Approach of 3M 45 at 2mm crack opening

Figure 5 shows a typical comparison of displacement along the fiber from the full finite element analysis and the semi-analytical approach. This particular result is for a 3M fiber with inclination angle of 45 degrees, and crack opening of 2mm. The Young's modulus for glass, fiber coating and polymeric matrix are respectively 72.4 GPa, 50 MPa and 4 GPa. In Figure 5, the z-axis represents distance along the original fiber direction (before bending) from the face of the crack. Negative values represent the part of fiber inside the crack. The x-axis represents displacement perpendicular to the original fiber axis. The corresponding plot of radius of curvature distribution is given in Figure 6. Here, the position along the horizontal axis represents the actual distance along the deformed fiber axis (the s-coordinate) measured from the inflection point. Note that the radius of curvature is infinite at the inflection point, and stays very high at the initial part of the plot. We have therefore started to plot the result when the radius of curvature has decreased to 50mm. Above this value, the optical loss in common optical fibers is usually negligible. From the results shown in Figures 5 and 6, it is clear that the results from the semi-analytical approach are in excellent agreement with those from the full finite element analysis. The much simpler analytical approach is hence adopted to perform the analysis in the present paper.

In this investigation, we focus on the development of crack sensor with single mode fibers. With only one propagation mode inside the fiber, Marcuse (1976) has derived an analytical expression relating the power loss per unit length to the fiber curvature, as well as other parameters that can be derived from the wavelength of light, the fiber optical properties and the fiber core size. For details of the analysis, the readers are referred to the original reference. It suffices to say that once the curvature distribution along the fiber is known, the loss at each curved section can be calculated. Integration can then be performed with Marcuse's equation (for loss per unit length vs curvature) to obtain the total loss along the bent fiber.

As a result of the photoelastic effect, the optical properties of glass will change when it is under stress. In Marcuse's derivation, the photoelastic effect is neglected, so the results are only theoretically correct for very small curvature, when the bending stresses are small. In our case, the finite element analysis shows that the radius of curvature can be on the order of 1 mm, and high stresses are induced in the fiber. As pointed out by several investigators (Nagano et al. 1978, Gauthier et al. 1997, Valiente et al. 1989), the photoelastic effect is essentially leading to a reduction in fiber curvature. Rather than incorporating the photoelastic effect into the analysis, an empirical reduction factor can be obtained from experimental testing. In our work, optical fibers are looped around cylindrical rods of different diameters (Fig. 7). The measured loss (per unit length) is compared

with theoretical prediction from Marcuse's model. The ratio of theoretical to experimental value gives the reduction factor. For different optical fibers, the reduction factor is not the same. In our work, based on experimental testing, the correction factors for two different types of optical fibers have been obtained.

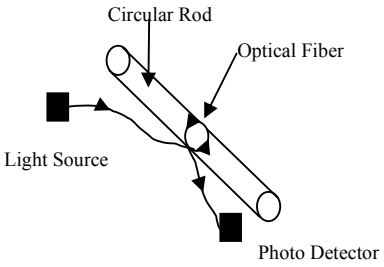

Figure 7. The Determination of Correction Factor for the Photoelastic Effect

4 SENSOR FABRICATION

The preparation of the optical fiber sensor is illustrated in Figure 8. With round pegs (which may be removed later) placed at proper locations inside a mould, the fiber is made to run in a pre-determined configuration. With the fiber held tight, polyester is poured slowly into the mold to form a sensor sheet several millimeters in thickness. Before polyester is added, releasing oil is added on all sides of the mold and the pegs, to facilitate removal of the sheet after the polyester hardens. Releasing oil is also put on the surface of the optical fiber. By minimizing the bond between the fiber and the polyester, when a crack in the concrete structure induces cracking of the sensor sheet, the fiber will be able to slide and bend to introduce optical power loss. Before the polyester hardens, fine sand particles are also added. These particles will sink into the polyester and make the hardened sheet more brittle. Once a crack in the concrete member intersects with the sheet, the sheet will crack at once. For applications requiring an externally bonded plate (e.g., monitoring of flexural cracks at the bottom of a bridge deck), the preparation procedure described above is sufficient. For an internally embedded sensor, stone aggregates are also added to the polyester before it hardens (as shown in Fig. 8). These aggregates, which protrude from the surface of the sensor sheet, will improve the bond when the sheet is embedded inside concrete. At the location where the fiber is coming out of the sheet, a small steel tube is placed around the fiber for protection and the end of the steel tube is further covered with soft rubber. This way, the breakage of fiber at the exit point can be prevented.

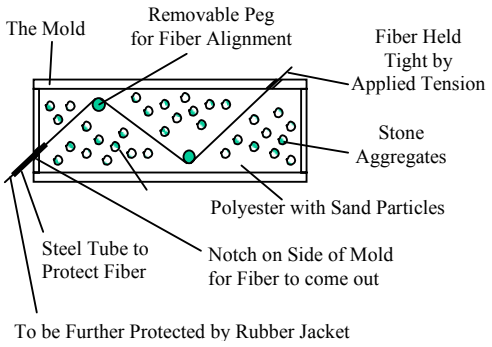

Figure 8. Illustration of the Fabrication a Sensor Sheet

5 EXPERIMENTAL RESULTS WITH THE CRACK SENSOR

5.1 Crack monitoring under monotonic loading and comparison with theory

As a first illustration of crack monitoring with the sensor sheet, a simple experiment involving the bending of a concrete beam is performed. The specimen and testing configuration is shown schematically in Figure 9. The sensor sheet is embedded inside the concrete beam at a distance from the bottom surface. A pair of notches is cut on the two sides of the beam, so the crack location is known. A LVDT is placed across the notch at the same level of the sensor sheet along the depth of the beam. When loading is applied, the optical power loss is measured simultaneously with the crack opening. A number of tests have been performed using sensor sheets made with different types of optical fibers running at different angles to the longitudinal direction. In Figure 10, the results for sensors made with SMF28 fibers running at 30 and 45 degrees to the crack plane are shown. (Note: for single mode propagation, a 1550 nm LED light source was employed in the experiment.) In the plots, the signal loss of the fiber was measured with an optical power meter, while the crack opening is obtained with the LVDT. Also shown in Figure 10 are the predicted power loss vs. crack opening relations from the model described in the last section. Generally speaking, the agreement between experimental and theoretical results is very good.

At large openings, the experimental results show oscillations in the power loss that are not present in the theoretical results. These oscillations are believed to be due to a stick-slip effect caused by friction at the optical fiber/polymeric interface. Despite the application of releasing oil on the fiber surface, friction cannot be completely eliminated. From a practical point of view, this should not be a major issue. Significant oscillation only occurs at relative large openings when the high power loss value should have already prompted the owner of the structure to take appropriate action. The 'error' in the output signal resulted from the oscillations is therefore not important.

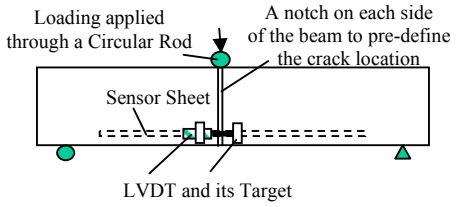

Figure 9. Test configuration to demonstrate the capability of the sensor sheet in the monitoring of internal crack

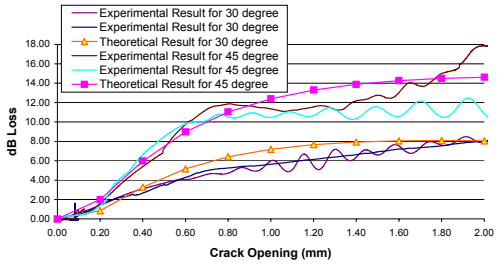

Figure 10. Experimental and Theoretical Results for Crack Sensors with SMF28 Fiber at 30 and 45 degrees to the Crack Plane

Both the theoretical and experimental results indicate that the sensitivity of the sensor to crack opening increases with the fiber inclination angle to the crack plane. If the sensor is designed for the monitoring of one or two cracks, a higher inclination angle should be employed. However, with a higher angle, the asymptotic loss at large crack opening is also higher. When a sensor is designed for the distributed sensing of a large number of cracks, one should limit the asymptotic loss so the dynamic range of the OTDR system will not be used up when light has passed through a small number of cracks. For different applications, different signal loss vs. crack opening relations are desirable. Using the theoretical model, which has been verified with experimental data, simulation can be performed to identify the appropriate design parameters (such as fiber type, inclination angle, fiber coating) before actual sensors are made and tested to verify the performance. The amount of trial and error testing can hence be significantly reduced.

5.2 Preliminary work on crack monitoring under cyclic loading

Since one major application of the sensor is to detect structural damage under seismic load, a preliminary experiment has been performed with a sensor sheet embedded inside a T-shaped reinforced concrete specimen simulating the beam-column joint (Fig. 11). In the specimen, shear stirrups in the joint region are deliberately removed so diagonal cracking is likely to occur under cyclic loading. As shown in the figure, the specimen is fixed to a rigid base. Loading is applied laterally on the top to introduce cyclic shear and bending on the joint. A pair of steel plates is employed to create a gap between the specimen and the rigid base, so the joint region is free to rotate under loading. Starting from cyclic loading of small magnitude, the loading is increased gradually until diagonal cracks are formed inside the joint region. The loading magnitude is then kept constant, and cyclic loading is continuously applied to widen the crack. During the test, the loading and optical power output are simultaneously monitored.

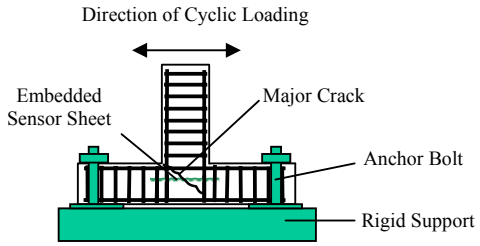

Figure 11. Specimen for Verification of Crack

5.3 Sensing during Cyclic Loading

Typical variation of optical power loss and loading with time are shown in Figure 12. The results are plotted in such a way that the values on the y-axis represent the loading (in kN) as well as the loss (in dB). As shown in the figure, the load undergoes full reversion in opposite directions (i.e., the maximum force in the two directions are the same. However,

as shown in Figure 11, only one major diagonal crack was found in the specimen. During about half of the cycle, the crack opens and the output from the sensor shows a loss. When loading is in the other direction, the crack closes up and the loss returns to zero. From the results, two interesting points can be noticed. Firstly, the loss is found to increase with the number of cycles, which reflects the increasing crack opening associated with continuous damage inside the joint region. Secondly, when the load goes to zero (from the negative side), a residual power loss remains. This residual loss also increases with the number of cycles. From a practical point of view, the residual loss can provide very useful information for the post-earthquake inspection of structures. Even when the sensor is not 'on-line' during the earthquake, an output from the sensor can be obtained after the event, in a remote manner with

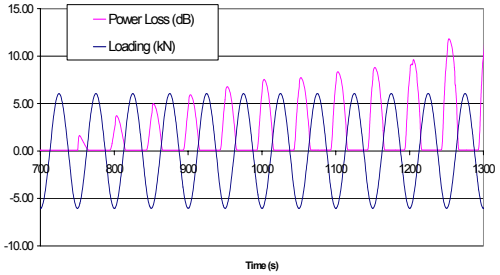

the OTDR system. Based on the magnitude of the loss, one can determine if a particular part of the structure has been severely damaged.

Figure 12. Variation of Power Loss and Loading with Time

6 CONCLUSIONS

In this investigation, the principle of a fiber optic crack sensor is presented. With this sensor, a single fiber can be employed to monitor a number of cracks, and the exact crack locations do not need to be known in a-priori. Actual sensors have been fabricated and tested. A theoretical model for power loss vs. crack opening is also developed. For crack sensing under monotonic loading, the predictions from the theoretical model are found to be in good agreement with experimental results. With its validity verified, the theoretical model can be employed to provide design guidelines for the crack sensor. Preliminary experimental work also shows that the sensor is applicable to crack monitoring under cyclic loading. Based on the experimental and theoretical results, the potential of the sensor for practical applications is demonstrated.

7 ACKNOWLEDGEMENTS

The work described in this paper was fully supported by a grant from the Research Grant Council of the Hong Kong Special Administrative Region, China (Project No. HKUST6196/01E).

8 REFERENCES

Marcuse, D. 1976, Curvature loss formula for optical fibers, *Journal of the Optical Society of America*, Vol.66, pp 216-220

Nagano, K., Kawakami, S., Nishida, S. 1978, Change of the refractive index in an optical fiber due to external forces, *Applied Optics*, Vol.17, pp 2080-2085

Valiente, I, Vassallo, C. 1989, New formalism for bending losses in coated single-mode optical fibers, *Electronics Letters*, Vol.25, pp.1544-1545

Gauthier, R.C., Ross, C. 1997, Theoretical and experimental considerations for a single-mode fiber-optic bend-type sensor, *Applied Optics*, Vol.36, pp 6264-6273

Leung, C.K.Y., Elvin, N., Olson, N., Morse, T.F. He, Y.-F. 2000, A novel distributed optical crack sensor for concrete structures, *Engineering Fracture Mechanics*, Vol.65, pp 133-148

Leung, C.K.Y. 2001, Fiber optic sensors for concrete structures: the future, *Non-destructive Testing and Evaluation*, Vol.34, pp 85-94

Olson, N., Leung, C.K.Y., Wang, X. 2002, Stiffness measurement of the external polymeric coating on optical fiber, *Experimental Techniques*, Vol.26, pp 51-56